Talanta 116 (2013) 548–553

Contents lists available at ScienceDirect

Talanta

journal homepage: www.elsevier.com/locate/talanta

Sensitive and selective detection of Ag^+ in aqueous solutions using Fe_3O_4@Au nanoparticles as smart electrochemical nanosensors

Huicui Yang [a,b], Xiaoxiao Liu [a,b], Ruihua Fei [a,b], Yonggang Hu [a,b,*]

[a] State Key Laboratory of Agricultural Microbiology, Huazhong Agricultural University, Wuhan 430070, China
[b] College of Life Science and Technology, Huazhong Agricultural University, Wuhan 430070, China

ARTICLE INFO

Article history:
Received 25 March 2013
Received in revised form
17 July 2013
Accepted 18 July 2013
Available online 26 July 2013

Keywords:
Fe_3O_4@Au nanoparticles
Ag^+
Magnetic
Electrochemical detection

ABSTRACT

Owing to the selective deposition reaction on the surface of magnetic nanoparticles, we reported a simple and selective magnetic electrochemical method for the detection of Ag^+ ions in aqueous solutions. The analyte deposited on the nanoparticles was brought to the surface of a homemade magnetic electrode and detected electrochemically in 0.1 mol/L KCl solution based on the reaction of Ag_0 transferred to AgCl. Under the optimal conditions, the linear response range of Ag^+ ions was 0.117–17.7 μmol/L (R^2=0.9909) with a detection limit of 59 nmol/L (S/N=3). A series of repeatability measurements 1.0 μmol/L Ag^+ gave reproducible results with a relative standard deviation (RSD) of 4.5% (n=11). The interference from other metal cations can be eliminated by adding EDTA as a co-additive to mask the metal cations. The recoveries ranging from 98.6% to 103.99% after standard additions demonstrate that this sensor has great potential in practical applications. The advantages of this developed method include remarkable simplicity, low cost, and no requirement for probe preparation, among others.

1. Introduction

Silver ions are considered to be one of the heavy metal ions. Its potential toxicity for environments and human body has drawn people attention. The Environmental Protection Agency (EPA) approves certification of silver as a pesticide (EPA 73499-2) and limits the discharge concentration of soluble silver to 5 ppm [1]. The standard safe concentration of Ag^+ for human is <0.05 ppm according to the World Health Organization (WHO) [2]. Traditional methods, such as inductively coupled plasma mass spectrometry (ICP-MS), flame atomic absorption spectrometry (F-AAS), atomic emission spectroscopy (AES), spectrophotometry, ion exchange chromatography (IEC) as well as laser excited atomic fluorescence spectrometry, had been used to detect trace levels of Ag^+ in aqueous media. However, these methods are normally performed in the laboratory and not suitable for on-site applications. Other drawbacks include the need for somewhat sophisticated and expensive instrumentation that can be time consuming to operate. The development of simple, low cost, sensitive and selective methods for detection of trace amounts of Ag^+ in environmental and food related samples is of great importance.

Owing to the advantages such as low cost, high sensitivity, straightforwardness, low sample volume, ease of operation and the ability to carry out speciation, electrochemical methods offer advantages for the determination of metal ions. There are several examples of electrochemical methods applied to the determination of Ag^+ in aqueous samples [3–14]. The performance such as the limit of detection and the linearity range of several electrochemical techniques for the detection of Ag^+ are summarized and compared in Table 1. Modified working electrodes were generally used to enhance the sensitivity and selectivity of electrochemical analysis techniques. The modifiers used include complexing reagents and special electrode-film coatings. The modification methods include chemisorption, covalent binding, polymer film coating, and composite. However, these methods for the determination of silver still suffer from more or less drawbacks such as the sophisticated pretreatment process, slow mass transport of the metal ions from bulk solution to the electrode surface, and matrix interferences, which limit their wide application [15,16].

Previous researches have been demonstrated that the incorporation of magnetic nanoparticles (MNPs) into sensors can enhance sensor performance [17–19]. First, the MNPs can be easily separated from the reaction mixtures with a magnet and re-dispersed immediately following removal of the magnet. It can effectively minimize the

* Corresponding author at: College of Life Science and Technology, Huazhong Agricultural University, Wuhan 430070, China. Tel.: +86 27 87280670; fax: +86 27 87280670.
E-mail addresses: yongganghu@163.com, yongganghu@mail.hzau.edu.cn (Y. Hu).

0039-9140/$ - see front matter © 2013 Published by Elsevier B.V.
http://dx.doi.org/10.1016/j.talanta.2013.07.041

Table 1
Comparison of performance for electrochemical detection of Ag^+.

Electrode	Method	Linear range	LOD	Ref.
DNA film modified gold electrode	EIS	100–800 nM	10 nM	[4]
Carbon paste electrode	ASV	0.05–150 μg L^{-1}	0.05 μg L^{-1}	[5]
LB/PAn-PTSA/GCE	LSSV	$6.0\times10^{\times-10}$–1.0×10^{-6} mol L^{-1}	4.0×10^{-10} mol L^{-1}	[6]
LB-TCA/GCE	DPASV	5.0×10^{-9}–2.0×10^{-6} mol L^{-1}	3.0×10^{-9} mol L^{-1}	[7]
Au-MBT SAM	SWV	5.0×10^{-8}–8.0×10^{-7} and 1.0×10^{-6}–1.0×10^{-5} M	1.0×10^{-8} M	[8]
CNTs/GCE	DPV	100 nM–2.5 μM	30 nM	[9]
MHA/SAM modified gold electrode	DPV	10–500 nM	1.3 nM	[10]

LB/PAn-PTSA/GCE: Polyaniline doped with p-toluenesulfonic acid Langmuir–Blodgett film modified glassy carbon electrode; LB-TCA/GCE: Langmuir–Blodgett film of p-tert–butylthiacalix [4] arene modified glassy carbon electrode; Au-MBT SAM: Gold 2-mercaptobenzothiazole self-assembled monolayer; CNTs/GCE: Carbon nanotubes modified glassy carbon electrode; MHA/SAM modified gold electrode: 16-mercaptohexadecanoic acid self-assembled monolayer modified gold electrode; EIS: Electrochemical impedance spectroscopy; ASV: Anodic stripping voltammetry; LSSV: Linear scanning stripping voltammetry; DPASV: Differential pulse anodic stripping voltammograms; SWV: Square wave voltammograms; DPV: Differential pulse voltammograms.

matrix effect from the samples. Second, the MNPs provide a larger surface area than that of a flat solid phase, thus permitting a large amount of analyte to be captured, leading to increased detection sensitivity. Third, the analyte can be captured by MNPs and then brought to a sensing surface by magnetic electrode for direct detection without the need for further processing. This can reduce the complexity and time required for the sensing application. Forth, MNPs and magnetic separators enabling automated handling of the MNPs are commercially available. Due to these advantages, several MNPs-based electrochemical methods for metal ions sensing have been recently presented by attaching the chelating reagents onto MNPs surface to effectively capture metal ions [20–23]. The selectivity of these methods above also depends on the binding interaction of metal ions and complexing agent.

Herein, we introduce a new concept of utilizing commercial Fe_3O_4@Au nanoparticles as the smart electrochemical nanosensors, which serve as the active element and direct electroanalytical quantification of analytes. The novelty of this work not only resides in the description of a chemical deposition process but also includes the ability to search, reduce, trap and detect Ag^+ ions from water in a selective manner. The schematic design is depicted in Scheme 1. (1) The Fe_3O_4@Au were dispersed into the sample and hence brought directly to the analyte. (2) The Ag^+ ions could be reduced to Ag_0 by the residual hydroxylamine groups on the surface of Fe_3O_4@Au composites, where the Fe_3O_4@Au acted as the catalyst. Meanwhile, the Ag_2O were also formed in aqueous base. Both species deposited on the surface of Fe_3O_4@Au nanoparticles. (3) The Fe_3O_4@Au was brought to the electrode surface by a magnetic electrode, then, the Ag_2O were electrochemically reduced to Ag_0. Finally, the amount of analyte was detected electrochemically in 0.1 mol/L KCl solution based on the reaction of Ag_0 transferred to AgCl.

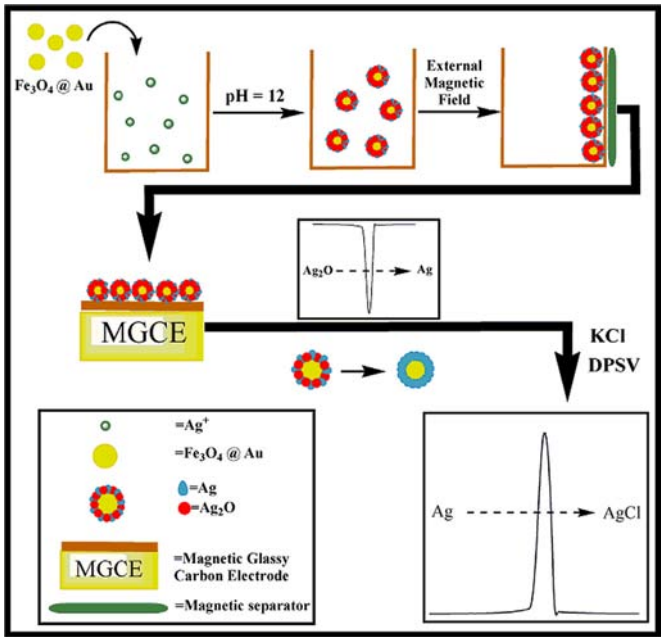

Scheme 1. Illustration of the procedure used to detect the Ag^+ ions in aqueous solution.

2. Experimental

2.1. Material and reagents

All reagents and chemicals were of analytical grade. A 0.117 mol/L stock solution of Ag^+ were prepared by dissolving the appropriate amounts of $AgNO_3$ (Merck, Germany), and were stored at 4 °C for further use. Fe_3O_4@Au nanoparticles (50 nm) and magnetic separation racks were purchased from Shanxi Life Gen Co., Ltd. (Xi'an, China).

2.2. Apparatus

Cyclic voltammograms (CVs) and differential pulse voltammetry (DPV) were performed in a Gaoss Union electrochemical analyzer (Wuhan, China). All measurements were carried out at room temperature (25 ± 1 °C) in a 2.5 mL electrochemical cell with a normal three-electrode configuration. A homemade magnetic glassy carbon electrode was used as working electrode [24]. A platinum wire counter electrode and a saturated calomel reference electrode (SCE) were used in the three electrodes configuration. The pH of all buffer solutions was measured by an Orion pH meter (United Initiators Co., Ltd., America). The solutions were prepared by the use of ultra pure water, which was obtained through a Cascada Lab Water System (USA). An Oscillator (Kylin–Bell Lab Instruments Co., Ltd., Jiangsu, China) was utilized to disperse magnetic particles.

2.3. Analytical procedure

Fe_3O_4@Au nanoparticles were firstly added into the samples and hence brought directly to the analyte. The pH of mixture solutions were then adjusted to 12.0, after which the mixture solutions were incubated for 5 min at room temperature. A magnetic separation rack was used to separate the magnetic particles from the solution phase, and the supernatant was discarded. The Fe_3O_4@Au nanoparticles were washed three times with ultra pure water to remove residual matrix.

The homemade glassy carbon (GC) magnetic electrode was used to capture Fe_3O_4@Au nanoparticles for the subsequent detection. The electrochemical events were performed in 0.1 mol/L KCl solution (pH=7.0). The Ag_2O deposited on the surface of Fe_3O_4@Au nanoparticles were electrochemically reduced to Ag_0 at a constant potential of −0.5 V for 120 s. The amount of Ag^+ was electrochemically detected based on the reaction of Ag_0 transferred to AgCl. The differential pulse voltammogram response (DPV) detection was performed from −0.2 to 0.4 V, with a step potential of 4 mV, a pulse amplitude of 50 mV, and a pulse period of 0.2 s.

3. Results and discussion

3.1. Characterization of the Ag^+ ions deposited on the surface of Fe_3O_4@Au nanoparticles

The approach to generation of Fe_3O_4@Au composites use hydroxylamine as reducing agents to deposit the Au nanoparticles on the nano-Fe_3O_4 surface, which result in residual hydroxylamine groups on the surface of Fe_3O_4@Au composites [25]. Fig. 1 shows cyclic voltammograms performed to determine the electrochemistry of the Fe_3O_4@Au nanoparticles in the presence and absence of Ag^+, once brought to the surface of a GC magnetic electrode. The positive scan shows an oxidation peak is attributed to oxidation of Ag to AgCl in 0.1 mol/L KCl (Fig. 1A). No current peaks were observed in the absence of Ag^+. The distinct peak observed in the presence of Ag^+ demonstrate clearly the ability of the Fe_3O_4@Au nanoparticles to capture the desired analyte and bring it back to the electrode to be detected. Results shown in Fig. 1A reveal that silver is electrochemically detected by being reduced to its metallic form Ag_0 and deposited on the surface of Fe_3O_4@Au nanoparticles. This is due to a combined role of the residual hydroxylamine groups as the reducing agent and Fe_3O_4@Au nanoparticles as the catalyst in the adsorption/deposition process of Ag^+ [26–28]. The oxidation peak current significantly increased when the sample pH was adjusted from 7.0 to 12.0 after the magnetic nanoparticles added into the sample solution (Fig. 1B), which suggested the basic condition of solution was value to the reductive reaction and the formation of Ag_0 on the nanoparticle surface.

During the negative scan, a reductive peak at +0.1 V was observed in the presence of Ag^+ ions (Fig. 1C). On the basis of previous studies, this is attributed to the electroreduction of Ag_2O to Ag_0 [29]. This indicates that the Ag^+ ions partly deposited on nanoparticle surface due to the formation of Ag_2O. Accordingly, we electrochemically reduced the Ag_2O to Ag_0 before the electrochemical detection of Ag^+ ions in sample. By this means, the oxidation peak current for oxidation of Ag_0 to AgCl could be further improved (Fig. 1D), which indicates the increase of the amount of Ag_0 on the magnetic nanoparticle surface.

3.2. Optimization of the experimental conditions

The effect on the electrochemical signal of the addition amount of Fe_3O_4@Au nanoparticles was investigated from 25 μg to 70 μg (Fig. 2A). An increase in the oxidation peak current was observed up to 50 μg. The large amount of Fe_3O_4@Au nanoparticles did not improve the sensitivity for electrochemical detection. The reason is probably due to the excess nanoparticles blocking the mass transformation, minimizing the electric conductivity. 50 μg of nanoparticles, therefore, were added to subsequent experiments.

The effect of sample pH with the range from 4.0 to 14.0 was studied. As can be seen in Fig. 2B, the signals for electrooxidation

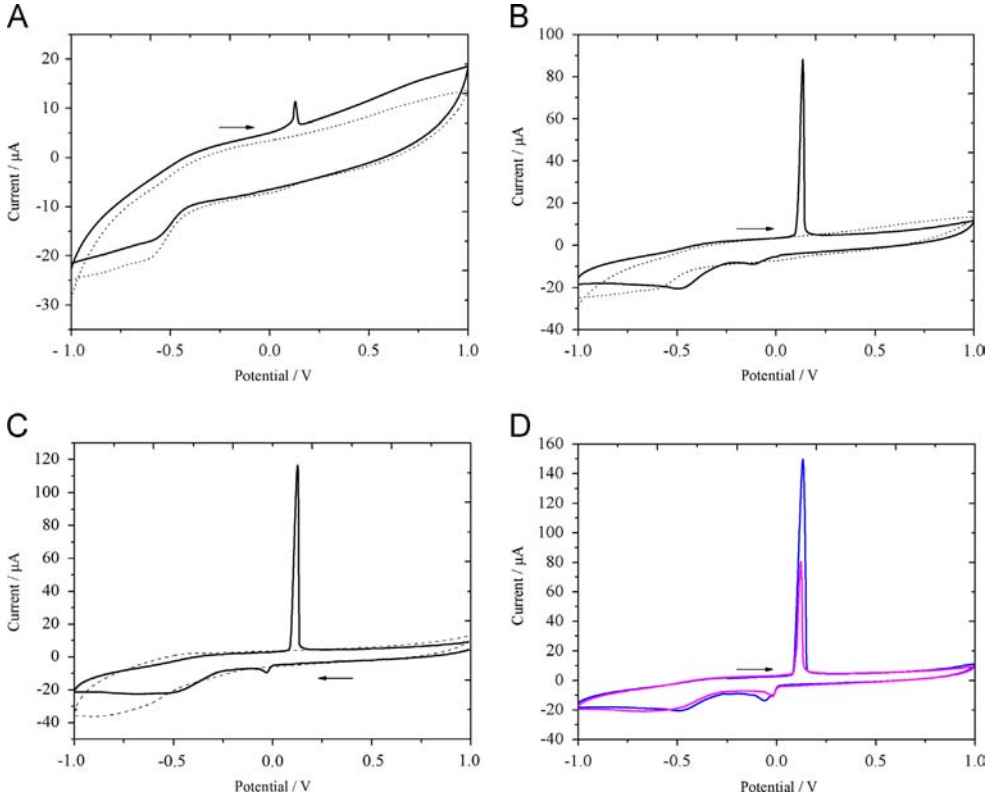

Fig. 1. Cyclic voltammograms obtained from Fe_3O_4@Au nanoparticles with (solid lines) and without (dashed lines) the deposition of silver. **A**, Fe_3O_4@Au nanoparticles were incubated with samples at pH 7.0. D, the silver deposited on the surface of Fe_3O_4@Au nanoparticles was respectively treated with (blue lines)/without (pink lines) electrochemical reduction; reduction voltage, −500 mV; reduction time, 120 s. B–D, Fe_3O_4@Au nanoparticles were incubated with samples at pH 12.0. The arrow indicates the scanning direction. Other conditions: Fe_3O_4@Au nanoparticles, 50.0 μg; $AgNO_3$, 11.8 μmol/L (1.0 mL); incubation time, 300 s; scan rate, 50 mV/s. (For interpretation of the references to color in this figure legend, the reader is referred to the web version of this article.)

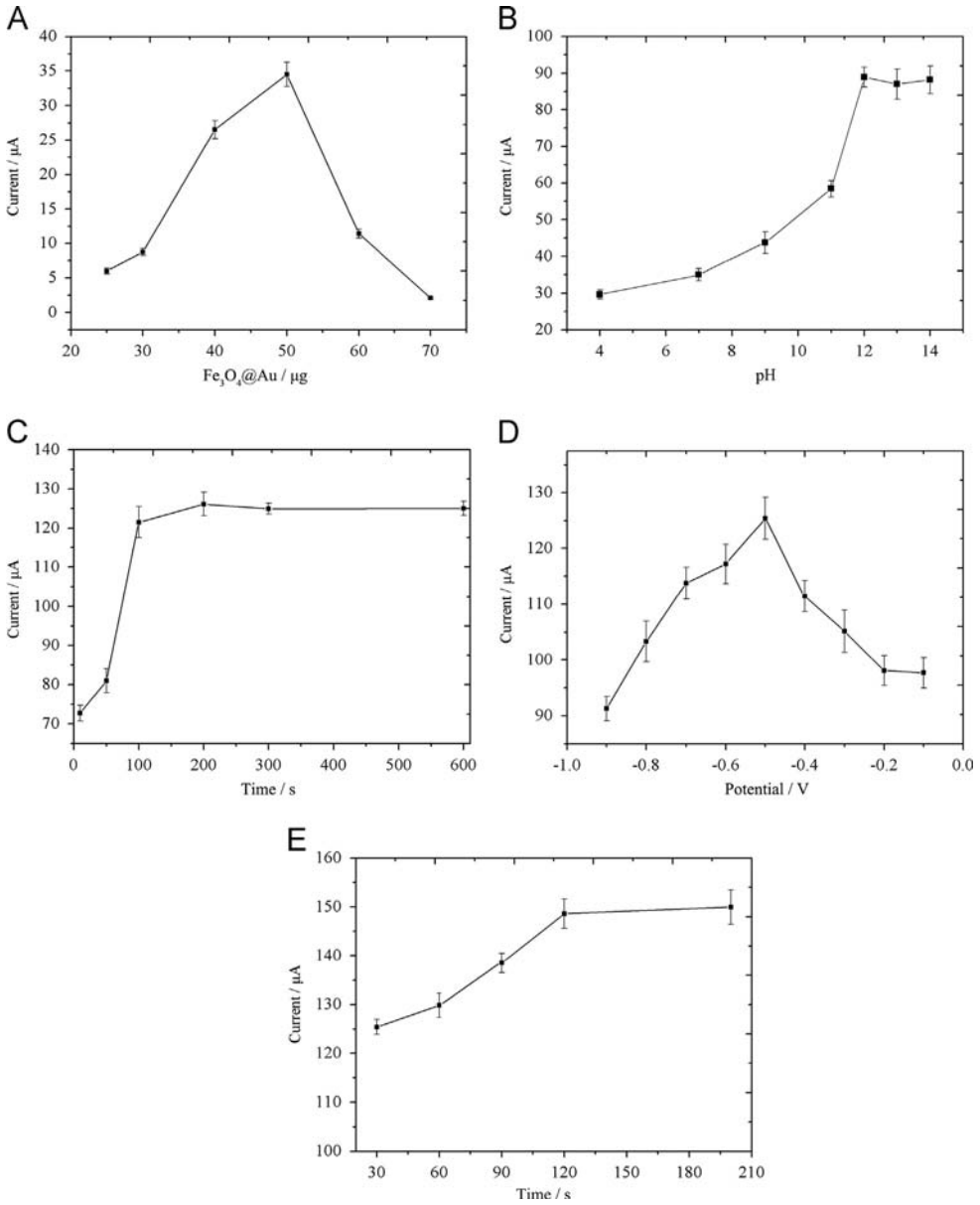

Fig. 2. (A) Effects of the amounts of Fe_3O_4 @ Au nanoparticles. Conditions: Fe_3O_4@Au nanoparticles were incubated with samples at pH 7.0; incubation time, 300 s; reduction voltage, −500 mV; reduction time, 30 s. (**B**) Influence of pH. Condition: incubation time, 300 s; reduction voltage, −500 mV; reduction time, 30 s. (**C**) Effects of incubation time. Conditions: Fe_3O_4@Au nanoparticles were incubated with samples at pH 12.0; reduction voltage, −500 mV; reduction time, 30 s. (**D**) Effects of reduction potential. Conditions: Fe_3O_4@Au nanoparticles were incubated with samples at pH 12.0; incubation time, 300 s; reduction time, 30 s. (**E**) Effects of reduction time on cyclic voltammograms. Conditions: Fe_3O_4@Au nanoparticles were incubated with samples at pH 12.0; incubation time, 300 s; reduction voltage, −500 mV. Other conditions: Fe_3O_4@Au nanoparticles, 50.0 μg; $AgNO_3$, 11.8 μmol/L (1.0 mL); scan rate, 50 mV/s. The error bars represent standard errors (SE) of the means. The data represent means ± SE (n=6).

of Ag_0 to AgCl were increased as pH increased from 4.0 to 12.0. Further increase of pH did not enhance the signal intensity. This indicates that the Ag^+ ions could be totally deposited on the surface of magnetic nanoparticles when the pH of sample solutions was adjusted higher than 12.0. Thus, pH 12.0 was selected for all subsequent experiments.

The current due to the oxidation of Ag_0 to AgCl is monitored as a function of incubation time in the sample solution. The current response reaches a stable value after approximately 200 s incubation. And 300 s was evaluated to be the optimum incubation time (Fig. 2C) to confirm that all Ag^+ ions could be deposited on the surface of nanoparticles. The Ag_2O should be transformed to Ag_0 under negative potential before oxidation detection for Ag_0 to AgCl. As can be seen in Fig. 2D, the reduction potential from −100 mV to −900 mV was investigated, and −500 mV was selected for the subsequent detection. Under this potential, the duration of the reductive reaction in the range of 30–180 s was also examined (Fig. 2E), and 120 s was evaluated to be the optimum time. The electrochemical detection could be accomplished within 7 min. This reveals that our developed method for Ag^+ detection has short response time.

3.3. Calibration curves, sensitivity, reproducibility and selectivity

Under the optimal conditions, the sensitivity of the developed electrochemical nanosensors was investigated. Different oxidation peak currents obtained in the DPV response after transformed Ag^+ to Ag_0 on the nanoparticle surfaces was tested. As shown in Fig. 3, the oxidation current of Ag_0 was linear with respect to the Ag^+ concentration in the sample solutions over the range 0.117–17.55 μmol/L.

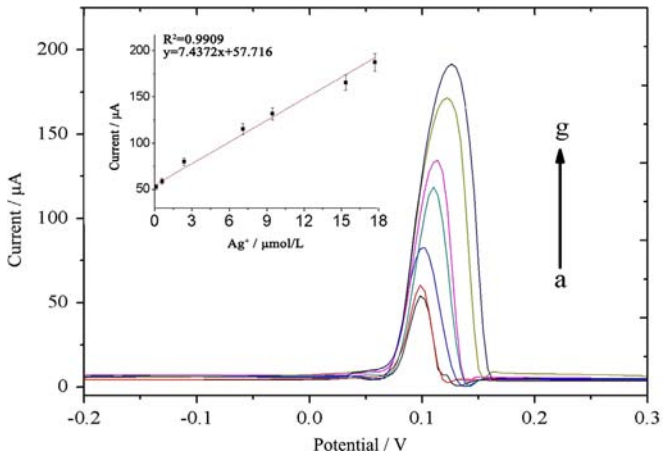

Fig. 3. Differential pulse voltammogram response with different concentrations of Ag^+ ions at optimal conditions. From a to g: the Ag^+ concentrations changed from 0.117 μmol/L to 17.550 μmol/L. The inset is the calibration curve for Ag^+ ions. The error bars represent standard errors (SE) of the means. The data represent means ± SE ($n=6$).

The regression equation was $Y=7.4372X+57.716$ (Y is the peak current and X is the concentration of Ag^+ ions in sample solution) with the regression correlation coefficient of 0.9909. The detection limit of this method was estimated as 59 nmol/L based on the signal-to-noise (the ratio of DPV response in the presence of Ag^+ to DPV response without Ag^+) characteristics of $S/N=3$ (where the S and N are the DPV response in the presence and absence of Ag^+, respectively), which is compared well with the reported results [8,9,30–32]. The limit of quantitation for silver ion using the proposed method was estimated to be 117 nmol/L based on the signal-to-noise characteristics of $S/N=10$. These indicate the proposed nanosesors can successfully detect Ag^+ in solution with a high sensitivity and low detection limit. Since WHO standard safe concentration for human is 0.05 ppm (460 nmol/L), which is located in the linear range of the proposed method (117 nmol/L–17.55 μmol/L), our method can be directly used for safe assessment of Ag^+ without dilution or enrichment of the sample. Eleven measurements of 1.0 μmol/L Ag^+ yielded a standard deviation (RSD) of 4.5%. This result demonstrates that this sensing system has a very good reproducibility.

The influence of co-existing metal ions on the determinations of 1.17 μmol/L Ag^+ was investigated under the above conditions. Fortunately, the addition of large amount of EDTA has no effect on the electrochemical detection of Ag^+. Therefore, the interfering effects could be avoided successfully by the addition of complexing agents EDTA into the sample solutions. 50 times of Ag^+ concentration of Ca^{2+}, Fe^{3+}, Pb^{2+}, Co^{2+}, Cd^{2+}, Mg^{2+}, Zn^{2+}, Cu^{2+} and Al^{3+}, and 5 times of Ag^+ concentration of Hg^{2+} did not exhibit interference when 58.5 μmol/L EDTA was added into the Ag^+ solution. The reason of the interference caused by high concentration of Hg^{2+} may be due to the Ag^+ and Hg^{2+} have similar reduction potentials (Ag^+/Ag_0, $E^0=0.80$ V; Hg^{2+}/Hg_0, $E^0=0.85$). These results above indicate that the method has a good tolerance to matrix interference.

3.4. Practical application of the Ag^+ sensing assay

Reliability was examined by recovery experiment in real samples (tap water) using the standard addition method. Then the concentration of Ag^+ in the samples was analyzed by the proposed method (Table 2). The recoveries ranging from 98.6% to 103.99% after standard additions are satisfactory, these results demonstrated that this sensor can be challenged by real water samples and has great potential in practical applications. The proposed electrochemical method was applied to the determination of Ag^+ in lake, tap and synthesized water samples. Ag^+ concentrations were obtained from a conventional calibration curve and following a standard addition methodology. As can be observed in Table 3, there is a good agreement between the results obtained from the developed electrochemical method and the results obtained when the same samples were analyzed by an alternative method (inductively coupled plasma-atom emission spectroscopy, ICP-AES), demonstrating the high potential of the novel electrochemical nanosensors for the analysis of Ag^+ in real samples.

Table 2
Recoveries for several Ag^+-spiked tap water.

Sample	Added (μmol/L)	Found (μmol/L) ($n=5$)	Recovery (%)
Tap water	0.351	0.355 ± 0.010	101.14
	1.404	1.460 ± 0.010	103.99
	2.925	2.930 ± 0.020	100.17
	5.850	5.960 ± 0.006	101.88
	12.870	12.690 ± 0.020	98.6

Table 3
Analytical results of Ag^+ in water samples obtained using the present electrochemical method and by inductively coupled plasma-atom emission spectroscopy (ICP-AES).

Sample	Original concentration (μmol/L)	Added (μmol/L)	Found (μmol/L) ($n=5$)	ICP-AES (μmol/L) ($n=5$)
Tap water	0	11.800	10.800 ± 0.029	11.050 ± 0.066
Lake water	0	5.900	6.130 ± 0.029	6.050 ± 0.051
Synthesized water	0.500	0.830	1.290 ± 0.048	1.330 ± 0.060

4. Conclusion

Based on the selective deposition of Ag^+ on the surfaces of commercial Fe_3O_4@Au nanoparticles, a novel and simple magnetic electrochemical method for the sensitive detection of Ag^+ has been demonstrated. This concept offers a new platform for the selective capture and detection of analytes. The matrix interference for the detection of Ag^+ caused by co-existing metal ions could be eliminated by the addition of complexing agents EDTA into the sample solutions. Compared with traditional electrochemical method, this developed method is more simple and economical for its low cost, easy preparation and time saving.

Acknowledgments

This work was supported by the Hi-Tech Research and Development Program of China (863 Program 2012AA101304), the National Natural Science Foundation of China (Grant no. 20005005), and the State Key Laboratory of Agricultural Microbiology, Huazhong Agricultural University (Grant no. AML-200905).

References

[1] C.L. Lasko, M.P. Hurst, Environ. Sci. Technol. 33 (1999) 3622–3626.
[2] F.K. West, P.W. West, T.V. Ramakrishna, Environ. Sci. Technol. 1 (1967) 717–720.
[3] C.-X. Tang, N.-N. Bu, X.-W. He, X.-B. Yin, Chem. Commun. 47 (2011) 12304–12306.
[4] Z. Lin, X. Li, H.-B. Kraatz, Anal. Chem. 83 (2011) 6896–6901.
[5] C. Labar, L. Lamberts, Talanta 44 (1997) 733–742.
[6] Q. Liu, F. Wang, Y. Qiao, S. Zhang, B. Ye, Electrochim. Acta 55 (2010) 1795–1800.
[7] F. Wang, Q. Liu, Y. Wu, B. Ye, J. Electroanal. Chem. 630 (2009) 49–54.

[8] R.K. Shervedani, M.K. Babadi, Talanta 69 (2006) 741–746.
[9] X. Liu, W. Li, Q. Shen, Z. Nie, M. Guo, Y. Han, W. Liu, S. Yao, Talanta 85 (2011) 1603–1608.
[10] G. Yan, Y. Wang, X. He, K. Wang, J. Su, Z. Chen, Z. Qing, Talanta 94 (2012) 178–183.
[11] M.B. Gholivand, M.H. Parvin, Electroanalysis 22 (2010) 2291–2296.
[12] J. Tashkhourian, S. Javadi, F.N. Ana, Mikrochim. Acta 173 (2011) 79–84.
[13] G. Jágerszki, A. Grün, I. Bitter, K. Tóth, R.E. Gyurcsányi, Chem. Commun. 46 (2010) 607–609.
[14] J. Zhao, Q. Fan, S. Zhu, A. Duan, Y. Yin, G. Li, Biosens. Bioelectron. 39 (2013) 183–186.
[15] I. Svancara, K. Kalcher, W. Diewald, K. Vytras, Electroanalysis 8 (1996) 336–342.
[16] D.E. Schildkraut, P.T. Dao, J.P. Twist, A.T. Davis, K.A. Robillard, Environ. Toxicol. Chem. 17 (1998) 642–649.
[17] K.Y. Chan, W.W. Ye, Y. Zhang, L.D. Xiao, P.H.M. Leung, Y. Li, M. Yang, Biosens. Bioelectron. 41 (2013) 532–537.
[18] B. Liu, D. Tang, B. Zhang, X. Que, H. Yang, G. Chen, Biosens. Bioelectron. 41 (2013) 551–556.
[19] S. Qu, J. Wang, J. Kong, P. Yang, G. Chen, Talanta 71 (2007) 1096–1102.
[20] I.Y. Goon, L.M.H. Lai, M. Lim, R. Amal, J.J. Gooding, Chem. Commun. 46 (2010) 8821–8823.
[21] W. Yantasee, K. Hongsirikarn, C.L. Warner, D. Choi, T. Sangvanich, M.B. Toloczko, M.G. Warner, G.E. Fryxell, R.S. Addleman, C. Timchalk, Analyst 133 (2008) 348–355.
[22] Q. Li, X. Zhou, D. Xing, Biosens. Bioelectron. 26 (2010) 859–862.
[23] Y. Wei, R. Yang, Y.-X. Zhang, L. Wang, J.-H. Liu, X.-J Huang, Chem. Commun. 47 (2011) 11062–11064.
[24] F. Li, L. Mei, Y. Li, K. Zhao, H. Chen, P. Wu, Y. Hu, S. Cao, Biosens. Bioelectron. 26 (2011) 4253–4256.
[25] Y. Cui, D. Hu, Y. Feng, J. Ma, Sci. China Ser. B-Chem 44 (2001) 404–410.
[26] K.V. Katok, R.L.D. Whitby, T. Fukuda, T. Maekawa, I. Be verkhyy, S.V. Mikhalovsky, A.B. Cundy, Angew. Chem. Int. Ed. 51 (2012) 1–5.
[27] G. Lai, F. Yan, F.J. Wu, C. Leng, H. Ju, Anal. Chem. 83 (2011) 2726–2732.
[28] I. Ojea-Jiménez, X. López, J. Arbiol, V. Puntes, ACS Nano 6 (2012) 2253–2260.
[29] P. Singh, K.L. Parent, D.A. Buttry, J. Am. Chem. Soc. 134 (2012) 5610–5617.
[30] R. Mikelova, J. Baloun, J. Petrlova, V. Adam, L. Havel, J. Petrek, A. Horna, R. Kizek, Bioelectrochemistry 70 (2007) 508–518.
[31] J.-H. Guo, D.-M. Kong, H.-X. Shen, Biosens. Bioelectron. 26 (2010) 327–332.
[32] S. Liu, J. Tian, L. Wang, X. Sun, Sensor. Actuat. B-Chem 165 (2012) 44–47.